On the spatial confinement in energy beam microprocessing

Nikita Arnold[a)]
Angewandte Physik, Johannes-Kepler-Universität, Linz, A-4040 Linz, Austria

The influence of nonlinearities in the absorptivity, heat conductivity, and chemical kinetics on the spatial resolution of patterns thermally produced by a focused energy beam is studied theoretically. It is shown that a decrease in substrate temperature and proper choice of processing temperatures can significantly improve the resolution. Example calculations are presented for Si. © *1995 American Institute of Physics.*

Energy beam microprocessing such as etching, deposition, doping, etc.,[1-3] is a convenient single-step technique for microelectronics and micromechanics in device fabrication. One of the goals to achieve is the improvement of the spatial confinement. The miniaturization of current microtechnology requires higher resolution which is limited by the wavelength of the energy beam used (laser beam, electron beam, etc.).

Several methods were used to increase the resolution in current energy beam processing. The localization of the processed zone can be significantly improved due to the nonlinear (Arrhenius) dependence of the reaction rate on temperature,[1,2] or by fast scanning for prenucleation combined with the use of an insulating layer which influences the resolution. Clearly, other linear and nonlinear effects can lead to either better or worse resolution. Sharpening due to changes in oxide layer absorptivity was studied theoretically.[4] Phase changes, latent heat release, and moving boundaries between different phases complicate the situation in laser annealing,[3,5] alloying, solidification,[6-7] amorphization,[8] and crystallization.[9] Here, even an approximate analytical consideration is practically impossible, and most of the studies were done numerically and/or for one-dimensional cases. In the present article we study analytically the influence of temperature dependences in the heat conductivity, the absorptivity, and the chemical reaction rate on the spatial resolution. We provide the optimal conditions for high-resolution processing and illustrate our statements for the example of silicon. The main result is that a decrease in workpiece temperature can significantly improve the resolution. The results can be applied mainly to the pyrolytic deposition, but also to dry etching and doping without material melting, which is not taken into account.

If the process used in application is thermally activated, the knowledge of the temperature distribution is a prior condition for any further considerations, in particular the spatial resolution. We consider a semi-infinite substrate irradiated by a focused energy beam with characteristic radius w_0. We assume the *constant* absorption coefficient α, which is a good approximation in *particle* beam processing.[10] The results also apply to arbitrary $\alpha(T)$, if absorption is *surface*, i.e., $\alpha^{-1} \ll w_0$. This is usually fulfilled for metals and semiconductors in the ultraviolet, and often in the visible spectral range, especially at elevated temperatures.[10,11] Note that the

finite penetration depth α^{-1} always widens the temperature distribution due to lateral spreading of the heat from the absorbing volume elements.

The distribution of the energy input $I(r)$ determines the temperature distribution $T(r)$. Because of the small spatial dimensions involved, the equilibrium is reached within the time $t \approx 10^{-4}-10^{-8}$ s and scanning of the energy beam does not impose a significant influence on the temperature distribution. Thus, it is enough to solve Laplace's equation for linearized temperature θ, given by the Kirchhoff transform.[12] We further assume that the temperature distribution directly determines the processing rate $W(r)$, i.e., we neglect any transport limitations.

If the absorptivity $A(T)$ is not a strongly decreasing function, the absorbed intensity $I_a = IA$, the temperatures θ and T, and the rate W are bell-shaped curves with different radii of localization w_i near $r=0$ (see Fig. 2). These quantities can be expressed via their maximum (central) values and the radii w_i as

$$I(r) \sim I_c(1 - r^2/w_0^2), \tag{1a}$$

$$A(r) \approx A_c(1 - r^2/w_A^2), \tag{1b}$$

$$I_a(r) \approx I_{ac}(1 - r^2/w_a^2), \tag{1c}$$

$$\theta(r) \approx \theta_c(1 - r^2/w_\theta^2), \tag{1d}$$

$$T(r) \approx T_c(1 - r^2/w_T^2), \tag{1e}$$

$$W(r) \approx W_c(1 - r^2/w_R^2). \tag{1f}$$

Clearly, these approximations hold only near the beam center, but with the good spatial resolution $w_R \ll w_0$ we are interested in, it is enough to study the behavior of these functions only in this region.

We want to calculate w_R for the given value of w_0. Because A, θ, and W depend only on temperature, we can use a Taylor expansion:

$$W(r) = W[T(r)] \approx W_c + \left.\frac{\partial W}{\partial T}\right|_{T=T_c} \Delta T(r)$$

$$\approx W_c \left(1 - \frac{T_c}{W_c}\left.\frac{\partial W}{\partial T}\right|_{T=T_c} \frac{r^2}{w_T^2}\right)$$

and therefore

[a)]Electronic mail: nikita.arnold@jk.uni-linz.ac.at

$$w_R^2 = w_T^2 \left(T_c \frac{\partial \ln W_c}{\partial T_c} \right)^{-1} . \tag{2a}$$

In analogy:

$$w_A^2 = w_T^2 \left(T_c \frac{\partial \ln A_c}{\partial T_c} \right)^{-1} , \tag{2b}$$

$$w_\theta^2 = w_T^2 \left(T_c \frac{\partial \ln \theta_c}{\partial T_c} \right)^{-1} . \tag{2c}$$

From $I_a = IA$, we derive

$$w_a^{-2} = w_0^{-2} + w_A^{-2} . \tag{3}$$

From a dimension analysis of the linear heat equation for θ it follows that:

$$w_\theta^2 = w_a^2 f(\alpha w_a) . \tag{4a}$$

The function f depends only on the geometry of the beam. For a Gaussian beam, which is a good approximation for an arbitrary bell-shaped curve,

$$f(\alpha w_a) = - \left(\frac{\partial}{\partial b} \ln \int_0^\infty \frac{e^{-b\xi^2/4} d\xi}{1 + \xi/\alpha w_a} \right)^{-1} \Bigg|_{b=1}$$

$$\approx \ln(1 + (0.06/\alpha w_a)^2) + 2 + \frac{2}{\alpha w_a + 0.45} . \tag{4b}$$

The first equality is derived from the general solution (5) for the surface temperature, induced by the stationary Gaussian beam,[12,13] and its second derivative at $r=0$:

$$\theta(r) = \frac{I_c A_c w_a}{2\kappa(T_0)} \int_0^\infty \frac{J_0(\xi r/w_a) e^{-\xi^2/4} d\xi}{1 + \xi/\alpha w_a} . \tag{5}$$

Here J_0 is the Bessel function, $\kappa(T)$ is the temperature-dependent heat conductivity, and T_0 the temperature far away from the irradiated zone. The latter approximation in Eq. (4b) is a fit based on the asymptotic behavior which holds with about 1% accuracy for all αw_a. Finally, we introduce the sharpening $s = w_R/w_0$, which is the ratio of radii of the reaction zone and the incident energy beam. It characterizes the spatial confinement. Smaller values of s correspond to better resolution. The equation for s can be readily found from (2)–(4):

$$s^2 = \frac{w_R^2}{w_0^2} = \left\{ f \left(\alpha w_0 \left(1 + s^{-2} \frac{\partial \ln A_c}{\partial T_c} \right/ \right. \right.$$

$$\left. \left. \frac{\partial \ln W_c}{\partial T_c} \right)^{-1/2} \right] \frac{\partial \ln \theta_c}{\partial T_c} - \frac{\partial \ln A_c}{\partial T_c} \right\} \Bigg/ \frac{\partial \ln W_c}{\partial T_c} . \tag{6}$$

With *surface* absorption $f=$const [e.g., $f=2$ in Eq. (4b)], and Eq. (6) gives *explicit* expressions for s. When θ_c, A_c, and W_c are known as functions of processing temperature, the optimal T_c which minimizes s can be chosen by changing the power of the energy beam.

Let us assume that the rate W is of Arrhenius type with an activation temperature T_a:

$$W(T) = k_o \exp(-T_a/T) , \tag{7}$$

linear dependence for the absorptivity,[11] and $\kappa(T)$ which is typical for semiconductors:

$$A(T) = A_0 + A_1 T , \tag{8}$$

$$\kappa(T) = \kappa(T_0)(T/T_0)^{-1-\epsilon} , \quad 0 < \epsilon < 1 . \tag{9}$$

Then the linearized temperature θ is

$$\theta(T) = \frac{T_0}{\epsilon} \left[1 - \left(\frac{T_0}{T} \right)^\epsilon \right] \tag{10}$$

and the derivatives in Eq. (6) are given by

$$\frac{\partial \ln A_c}{\partial T_c} = \frac{A_1}{A_0 + A_1 T_c} = \frac{A_1}{A_0 + \tau A_1 T_0} ,$$

$$\frac{\partial \ln W_c}{\partial T_c} = \frac{T_a}{T_c^2} = \frac{T_a}{T_0^2} \tau^{-2} , \tag{11}$$

$$\frac{\partial \ln \theta_c}{\partial T_c} = \frac{\epsilon T_c^{-1}}{(T_c/T_0)^\epsilon - 1} = \frac{\epsilon \tau^{-1} T_0^{-1}}{\tau^\epsilon - 1} .$$

In the second equalities we introduced the dimensionless temperature $\tau = T_c/T_0$.

The minimization of s depends on the particular experimental situation. An increase in A with temperature leads to the sharpening effect, while a decrease in A, or $\alpha^{-1} \neq 0$, results in delocalization of the reaction zone. T_a depends on the type of chemical reactions involved and sometimes can be changed by changing precursor or etchant molecules (clearly, with other parameters kept constant, T_a should be increased[1]). If T_c should be kept above a certain value (for example, because of the small reaction rate) then it is better to diminish T_0. For constant A and surface absorption ($f = 2$) with T_0 kept constant, for each material characterized by ϵ there exists an optimal processing temperature T_c (dependent on T_0), given by differentiation of Eq. (6) with the help of Eq. (11):

$$T_{c\,opt} = T_c \tau_{opt} = T_0 (1 - \epsilon)^{-1/\epsilon} , \tag{12a}$$

with the maximum possible sharpening

$$s_{opt} = \left[\frac{2T_0}{T_a} (1 - \epsilon)^{1 - 1/\epsilon} \right]^{1/2} . \tag{12b}$$

The resolution increases with increasing ϵ (more pronounced changes in the heat conductivity). For the limiting cases $\epsilon = 0$ and $\epsilon = 1$ we find $s_{opt}(0) = (2eT_0/T_a)^{1/2}$ and $s_{opt}(1) = (2T_0/T_a)^{1/2}$, respectively. With the approximations made, the optimal processing temperature $T_{c\,opt}$ does not depend on T_a and scales linearly with T_0. To improve the spatial confinement one should try to diminish T_0. The lowering of T_0 can cause several problems. Among those—increasing complexity of the experimental setup, too low T_0 for the handling of the chemicals used, the decrease in $T_{c\,opt}$ can significantly slow down the overall processing rate.

We shall apply the above treatment to c-Si substrates with $\kappa(T) = 1.62 \times 10^3 \, T^{-1-\epsilon}$ W/cm K with $\epsilon = 0.22$.[14] As an illustrative example we consider pyrolytic decomposition of SiH_4 with an activation temperature $T_a \approx 2.3 \times 10^4$ K.[15] Clearly, with very low substrate temperatures this particular reaction can hardly be used for practical purposes because of
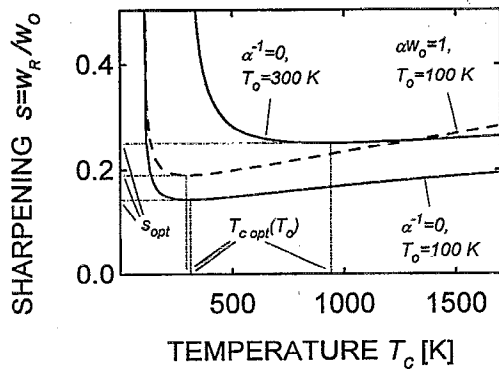
Nikita Arnold

FIG. 1. Dependence of sharpening s on processing temperature T_c for two substrate temperatures, T_0. The parameter values correspond to the deposition of Si from SiH_4 on the c-Si substrate: $\kappa(T) = 1.62 \times 10^3 \, T^{-1.22}$ W/cm K, $A_0 = 0.5$, $T_a = 2.3 \times 10^4$ K, $w_0 = 1$ μm. Solid lines—surface absorption $\alpha^{-1} = 0$, with $A_1 = 0$. Dashed line—finite absorption $\alpha w_0 = 1$, with $A_1 = -5 \times 10^{-5}$ K^{-1}.

FIG. 2. Normalized intensity and reaction rate for different values of T_c and T_0 calculated from Eqs. (5), (7), and (10). Curve I—$\alpha^{-1} = 0$, $T_a = 300$ K, $T_c = T_{c\,opt}(300 \text{ K}) = 928$ K, $P = 327.5$ mW. Curve II—$\alpha w_0 = 1$, $T_0 = 100$ K, $T_c = 928$ K, $P = 1351$ mW. Curve III—$\alpha^{-1} = 0$, $T_0 = 100$ K, $T_c = 928$ K, $P = 734.4$ mW. Curve IV—$\alpha^{-1} = 0$, $T_0 = 100$ K, $T_c = T_{c\,opt}(100 \text{ K}) = 309$ K, $P = 416.7$ mW. $A_1 = 0$, and thus in Eq. (5) $w_a = w_0$ for all curves. Other parameters are the same as for Fig. 1.

the small vapor pressure of SiH_4 (3.5 mbar at 100 K[16]) and, as a consequence, the low processing rate. Nevertheless, the qualitative picture remains valid for other reactions and temperature intervals.

Figure 1 shows the dependence of s on T_c for $T_0 = 300$ K and $T_0 = 100$ K, as calculated from Eq. (6). The advantage in using lower T_0 is clearly seen. The optimal processing temperature for $T_0 = 100$ K is lower, $\tau_{opt} = 3.09$ in both cases with surface absorption [see Eq. (12a)]. The minimum in $s(T_c)$ curves is so shallow, that even if $T_c > T_{c\,opt}$, the use of lower T_0 is advantageous. This is important from a practical point of view, because $T_{c\,opt}$ for $T_0 = 100$ K is too low for technological purposes. However, even at the same processing temperature, T_c, a substrate temperature $T_0 = 100$ K allows significantly higher resolution to be achieved. The dashed curve was calculated for *finite* absorption with $\alpha w_0 = 1$ and $A_1 \neq 0$. With typically small values[11] of the coefficient A_1 in Eq. (8), the decrease in resolution is mainly due to finite absorption.

To check the accuracy of our approximations we show in Fig. 2 the normalized intensity and reaction rate distributions. We used the analytical solution Eq. (5). The temperature and the reaction rate were recalculated from Eqs. (10) and (7). The parameter values are included in the figure caption. Note the differences in the beam power P which were necessary to provide the indicated processing temperatures. Curve IV, which corresponds to $T_{c\,opt}$ for $T_0 = 100$ K, is included to illustrate the relatively small influence of T_c.

Figure 2 confirms the values of s given in Fig. 1 and earlier predictions. The width of the temperature distribution, and therefore the reaction rate distribution, becomes narrower for lower temperatures T_0 and widens for finite absorption. The sharpening of the temperature distribution is due to the fact that the hot area of the semiconductor in the center has a lower heat conductivity and acts as a thermal insulator. This effect is more important for lower tempera-
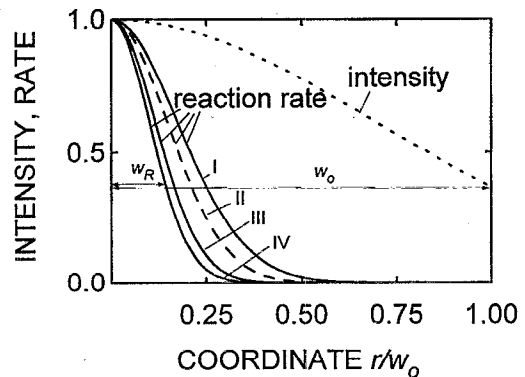
tures T_0 because the *relative changes* in heat conductivity become more pronounced.

Simple analytical formulas which take into account the influence of chemical kinetics, temperature dependences in the heat conductivity and absorptivity, as well as finite penetration depth on the spatial resolution of thermally produced patterns are provided. It is demonstrated that with semiconductors and crystalline insulators, where the heat conductivity decreases with increasing temperature, a decrease of the substrate temperature can result in a significant increase in resolution. Calculations are presented for the example of deposition on the silicon substrate. The results apply also to pyrolytic etching, and doping below melting threshold.

[1] D. Bäuerle, *Chemical Processing with Lasers* (Springer, Berlin, 1986).

[2] D. J. Ehrlich and J. Y. Tsao, *Laser Microfabrication: Thin Film Processes and Lithography* (Academic, New York, 1989).

[3] *Rapid Thermal Annealing/Chemical Vapor Deposition and Integrated Processing*, edited by D. Hodul, J. C. Gelpey, M. L. Green, and T. E. Seidel, Proc. MRS, Vol. 146 (North Holland, New York, 1989).

[4] N. A. Kirichenko and B. S. Luk'yanchuk, Sov. J. Quantum Electron. **10**, 819 (1983).

[5] R. F. Wood and G. A. Geist, Phys. Rev. B **34**, 2606 (1986).

[6] B. Basu and A. W. Date, Int. J. Heat Mass Transfer **33**, 1149 (1990).

[7] A. Kar and J. Mazumder, J. Appl. Phys. **68**, 3884 (1990).

[8] I. D. Calder and R. Sue, J. Appl. Phys. **53**, 7545 (1982).

[9] H. J. Zeiger, J. C. C. Fan, B. J. Palm, R. L. Chapman, and R. P. Gale, Phys. Rev. B **25**, 4002 (1982).

[10] G. K. Celler, CRC Crit. Rev. Solid State Mater. Sci. **12**, 193 (1984).

[11] G. E. Jellison, Jr. and F. A. Modine, Phys. Rev. B **27**, 7466 (1983).

[12] M. Lax, Appl. Phys. Lett. **33**, 786 (1978).

[13] M. Lax, J. Appl. Phys. **50**, 3919 (1977).

[14] C. J. Glassbrenner and G. A. Slack, Phys. Rev. A **134**, 1058 (1964).

[15] D. Bäuerle, P. Irsigler, G. Leyendecker, H. Noll, and D. Wagner, Appl. Phys. Lett. **40**, 819 (1982).

[16] *Gas Encyclopedia* (Elsevier, Amsterdam, 1976).